

# Surface-Mounted Smart PZT Sensors for Monitoring Damage Using EMI-Based Multi-Sensing Technique <sup>†</sup>

Aditya Parpe <sup>\*</sup> and T. Jothi Saravanan

School of Infrastructure, Indian Institute of Technology Bhubaneswar, Odisha, India; tjs@iitbbs.ac.in

<sup>\*</sup> Correspondence: ap35@iitbbs.ac.in; Tel.: +91-9315544507<sup>†</sup> Presented at the 8th International Electronic Conference on Sensors and Applications, 1–15 November 2021; Available online: <https://ecsa-8.sciforum.net>.

**Abstract:** In this article, the proposal of the multi-sensing technique on the surface-mounted PZT sensors is offered. The investigation is performed on the concrete structures for detecting and localizing the structural damage. Multiple smart sensing units (SSU) are adhesively bonded on the top surface of the concrete beam. As each PZT sensor has a small zone of influence, therefore, the use of multiple smart sensors is recommended for effective damage detection. The conductance signatures are obtained at different stages in the frequency range of 0–450 kHz. This article also presents the effective methodology for damage localization, which assumes the parallel connection of SSUs under MISO mode. The methodology adopted for structural damage detection is effective, as it is verified with the experimental results performed on the concrete structures with multiple surface-mounted PZT sensors.

**Keywords:** structural health monitoring; EMI; damage detection; PZT sensor; multi-sensing technique

**Citation:** Parpe, A.; Saravanan, T.J. Surface-Mounted Smart PZT Sensors for Monitoring Damage Using EMI-Based Multi-Sensing Technique. *Eng. Proc.* **2021**, *3*, x. <https://doi.org/10.3390/xxxxx>

Academic Editor:

Published: 1 November 2021

**Publisher's Note:** MDPI stays neutral with regard to jurisdictional claims in published maps and institutional affiliations.



**Copyright:** © 2021 by the authors. Submitted for possible open access publication under the terms and conditions of the Creative Commons Attribution (CC BY) license (<https://creativecommons.org/licenses/by/4.0/>).

## 1. Introduction

Smart materials are known for their ability to couple between multiple physical domains. They are widely used for the effective monitoring of structures [1]. Lead Zirconate Titanate (PZT) is known as the self-sensing material as it can act as an actuator and sensor. PZT sensor involves electro-mechanical (EM) coupling. Based upon EM coupling between the sensor and the structure, the electro-mechanical impedance (EMI) technique is proven to be promising for effective structural health monitoring (SHM). The EMI measurements are obtained from adhesively bonded PZT sensors to examine the changes caused due to damage [2,3]. The damage diagnosis [4] is the main objective behind using the EMI technique. Also, the embedded PZT sensors are famous for monitoring the early-age strength of concrete structures [5,6].

Researchers have performed numerical [7] and analytical [8] studies based upon adhesively bonded PZT sensors. The numerical approach utilizes coupled field analysis (CFA) through Finite Element Modeling (FEM). The researchers have studied the sensitivity of PZT sensors for damage detection in concrete structures for the studies based upon damage detection. Generally, structural damage is observed as cracks, deterioration, and holes in the structure. The conductance signatures obtained at various stages are compared to notice the changes caused due to damage [9], and to quantify the changes among signatures, damage indices [10] are preferred. Whenever the external load goes beyond threshold values, damage occurs. The multiple PZT sensors bonded on the structure help monitor the damage [11,12]. The availability of multiple PZT sensors also helps localize the damage in the structures. Therefore, the researchers have proposed the idea of a multi-sensing technique to avoid ambiguity [13].

The current research focuses on damage detection and localization in concrete structures using the multi-sensing technique. Investigation on the adhesively bonded smart

PZT sensors is carried out using CFA through FEM. The parallel/serial connection of smart PZT sensors must be made under MISO mode for the proposed localization method. The methodology adopted for structural damage detection is validated with the experimental studies. The trend of numerical and experimental results is compared to observe the correlation between them.

## 2. Methodology and Investigation

### 2.1. Introduction of Smart Sensing Units (SSUs)

Previous research [13] has shown the high sensitivity of SSUs to sense the changes caused due to damage. The SSU consists of a PZT patch, adhesive layer (RS epoxy), and mild steel plate. For the current research, the varying thicknesses of SSUs are taken. The steel plates sized 21 mm × 21 mm with varying thicknesses (0.75 mm, 1.5 mm, and 3 mm) are used. The PZT patch and adhesive layer size are 10 mm × 10 mm × 0.3 mm and 10 mm × 10 mm × 0.1 mm. The properties of PIC 151 are considered for the PZT patch. For FE simulation of SSUs, various in-built elements are used. The mesh size of the whole SSUs is taken as 1 mm. The top and bottom nodes of the PZT patch are given input voltage as 1 V and 0 V, respectively, and are coupled with the 'VOLT' DOF to allow the current flow. These SSUs are harmonically excited in the high-frequency range of 0–450 kHz. The resonant frequencies of each SSU are distinct as different thick plates are used., as shown in Table 1.

**Table 1.** Data showing resonant frequency for each SSU.

SSU No.	1	2	3
Thickness (mm)	0.75	1.5	3
Resonant frequency (kHz)	335	350	355

### 2.2. Investigation on the Concrete Beam with Multiple SSUs

The simply-supported concrete beam sized 100 × 100 × 1000 mm is taken. Multiple SSUs are surface-mounted on a concrete beam to monitor the structural performance. The beam is also subjected to external loading. The load impactor is used to apply point load at 530 mm away from support 1. Figure 1 shows the FE model of the concrete beam. The load of 10 kN and 30 kN load magnitudes are considered in the study. The damage (crack) is introduced at location 300 mm away support 1. The nodes of the lower part of the beam are merged to introduce a crack of length 20 mm.

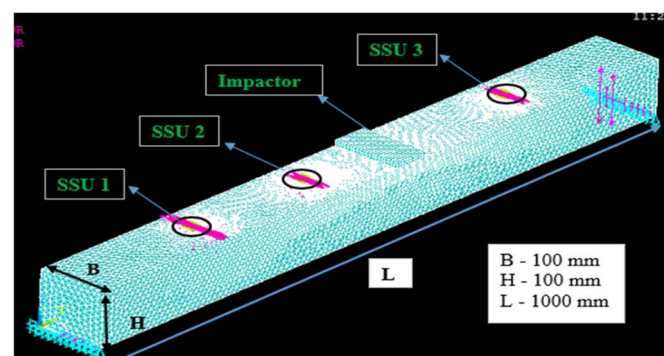


**Figure 1.** FE model of the simply-supported concrete beam with multiple SSUs.

Table 2 shows the data consists of the distance of load impactor and crack location from each SSU. The SSU-1 and SSU-2 are the farthest and nearest to the impactor, respectively. While the SSU-1 is nearest to the crack location, and SSU-3 is the farthest. The mesh size for beam and impactor is taken as 25 mm and 5 mm for numerical simulation, respectively.

**Table 2.** Data showing the distance of load impactor and crack location from each SSU.

SSU No.	1	2	3
Distance from impactor (mm)	310	110	250
Distance from crack location (mm)	70	120	480

### 2.2.1. Methodology for Structural Damage Detection

For the given numerical model of the concrete beam, the SSUs are harmonically excited in the frequency range of 0–450 kHz. The conductance signatures are obtained from each SSU at different stages and compared to examine the possible changes caused. The various damage indices, namely root mean square deviation (RMSD) and correlation coefficient (CC), quantify the changes among signatures.

### 2.2.2. Methodology for Structural Damage Localization

The multi-sensing technique is implemented on the surface-mounted SSUs. For parallel connection of sensors, the equivalent impedance ( $Z$ ) and admittance ( $A$ ) are expressed as  $Z_p = \sum_{i=1}^n \frac{1}{Z_i}$  and  $A_p = \sum_{i=1}^n A_i$ , respectively. Similarly for the serial connection of sensors, the equivalent impedance and admittance are expressed as  $Z_s = \sum_{i=1}^n Z_i$  and  $\frac{1}{A_s} = \sum_{i=1}^n \frac{1}{A_i}$ , respectively. As observed, the equivalent admittance in parallel connection is relatively higher, making it easy to identify the peaks in the composite signature. Therefore, the parallel connection of SSUs is assumed to obtain composite signatures. The dynamic metrics, namely, moving RMSD and moving CC, have been used for the localization process. These metrics are evaluated for the composite signatures obtained for a particular combination in the moving frame of 50 data points. The combinations as couplets (SSU 1-3, SSU 2-3) and triplet (SSU 1-2-3) are considered to get the approximate idea about damage location.

## 3. Results and Discussion

### 3.1. Detecting the Structural Damage

The conductance signatures are obtained for the pristine and damaged state of the beam to examine the presence of damage. Figure 2 shows the signatures obtained from each SSUs in the frequency range 200–450 kHz. Figure 2a shows that SSU-1 has detected the major changes caused due to inclusion of crack. In comparison, the SSU-2 and SSU-3 seem to be insensitive to the damage, as observed in Figures 2b,c. As damage is in the proximity of SSU-1, that's why SSU-1 is sensitive to the damage. Figure 3 shows the various statistical metrics evaluated for each SSU concerning the damage state. These metrics also infer that the SSU-1 has detected the major changes.

### 3.2. Localizing the Structural Damage

Figure 4 shows the moving RMSD plots for the different combinations of SSUs. For combination SSU 2-3, the magnitude of moving RMSD is higher at 350 kHz (SSU-2) than at 355 kHz (SSU-3). This indicates that conductance variation near SSU-2 is greater than SSU-3. It is found that the load impactor is nearby to the SSU-2, which is verified from Table 2. Similarly, for combination SSU 1-3, the magnitude of moving RMSD near SSU-1 is higher than SSU-3. As observed in the above statistical data, SSU-1 detected the influence of damage.

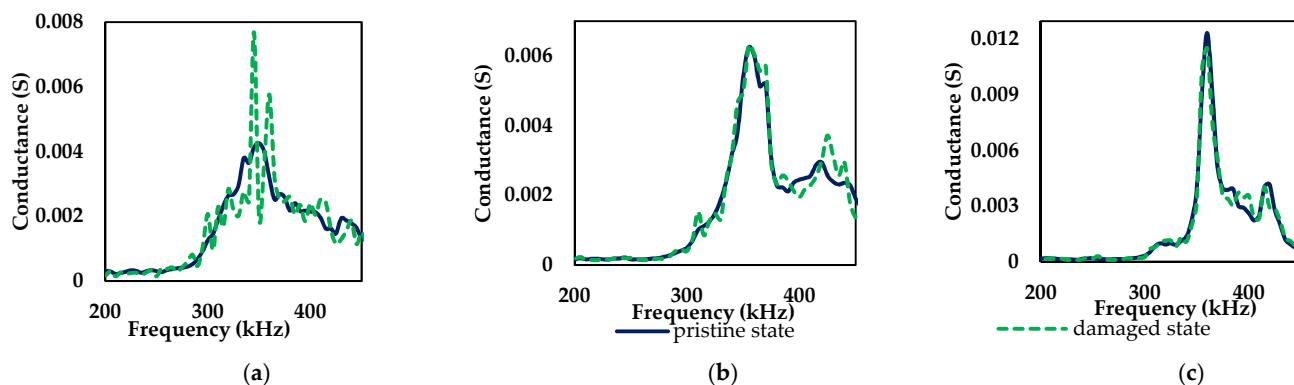


Figure 2. Conductance signatures obtained from (a) SSU-1; (b) SSU-2; (c) SSU-3 for the damaged concrete beam.

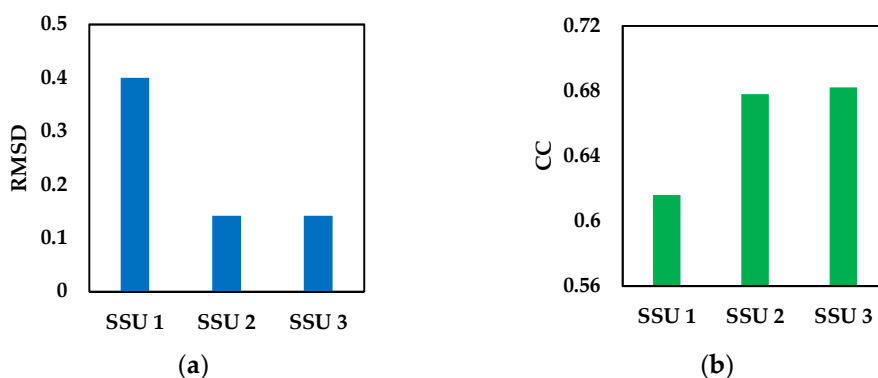


Figure 3. Various statistical metrics (a) RMSD; (b) CC evaluated for each SSU.

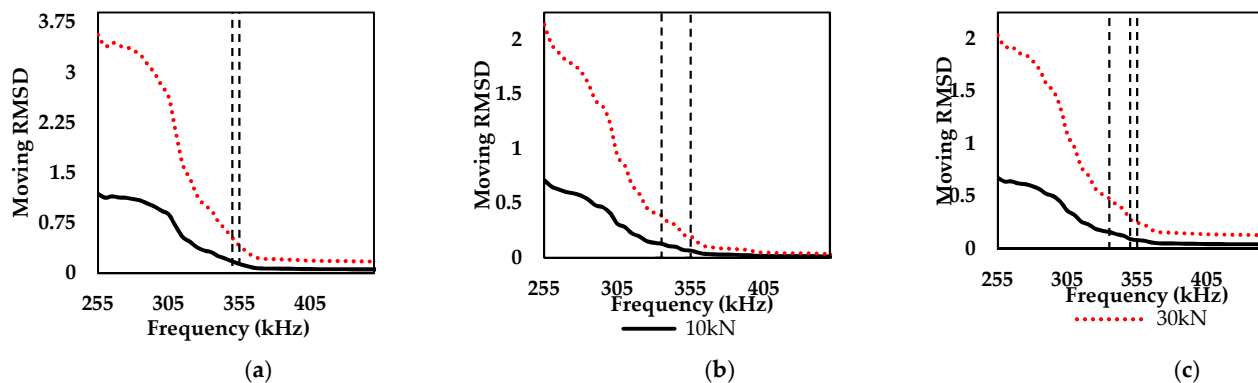


Figure 4. Moving RMSD plots for the combination (a) SSU 2-3; (b) SSU 1-3; (c) SSU 1-2-3 under different loading.

The moving RMSD plot for triplet SSU 1-2-3 shows that neither load impactor nor damage location is near the SSU-3. To verify the inferences observed from moving RMSD plots, another dynamic metric, i.e., moving CC, is evaluated for the different combinations of SSUs. Figure 5 shows the moving CC plots for different combinations of SSUs. Here, the magnitude of moving RMSD near SSU-2 is lower than SSU-3 for the combination SSU2-3. At the same time, the moving CC variation nearby to SSU-1 is lower than SSU-3. This verifies that the location of the load impactor is nearby to SSU-2, whereas the damage location is nearby to SSU-1. It also infers that SSU-3 is not able to detect neither load nor damage.

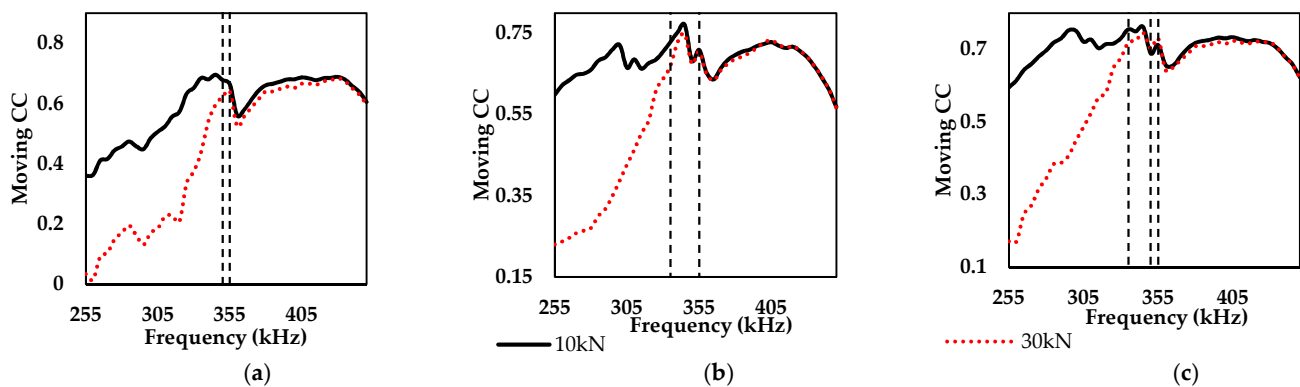


Figure 5. Moving CC plots for the combination (a) SSU 2-3; (b) SSU 1-3; (c) SSU 1-2-3 under different loading.

#### 4. Experimental Validation

The experimental studies are performed on the plain concrete beam sized 100 mm × 200 mm × 2000 mm. Three PZT sensors are bonded on the concrete beam, as shown in Figure 6. The sensors PZT-1, PZT-2, and PZT-3 are surface-mounted at 135 mm, 790 mm, and 1600 mm from the left end of a beam, respectively. For study based on damage detection, various damage cases are introduced in the beam. For validation work, two damage cases are considered [9]. Damage case-1 considers the inclusion of a 10 mm long crack at 210 mm from the left end of the beam. Here, the PZT-1 is nearest to the first crack location, whereas PZT-3 is the farthest one. Damage case-2 considers the inclusion of a 28 mm long crack at 858 mm from the left end of the beam. Here, the PZT-1, PZT-2, and PZT-3 are 723 mm, 68 mm, and 742 mm away from the second crack location. Using an impedance analyzer, all PZT sensors are excited harmonically in the frequency range of 30–100 kHz. Accordingly, the conductance signatures are measured for various PZT sensors at different states. Figure 7 shows the conductance variation measured for all PZT sensors. Here, PZT-1 has detected the major changes caused due to the inclusion of the first crack, whereas, other PZT sensors are insensitive to the first crack location. The statistical data shown in Figure 8, also infers that the first crack and second crack have been detected well by PZT-1 and PZT-2, respectively.



Figure 6. Plain concrete beam with multiple surface-mounted PZT sensors [9].

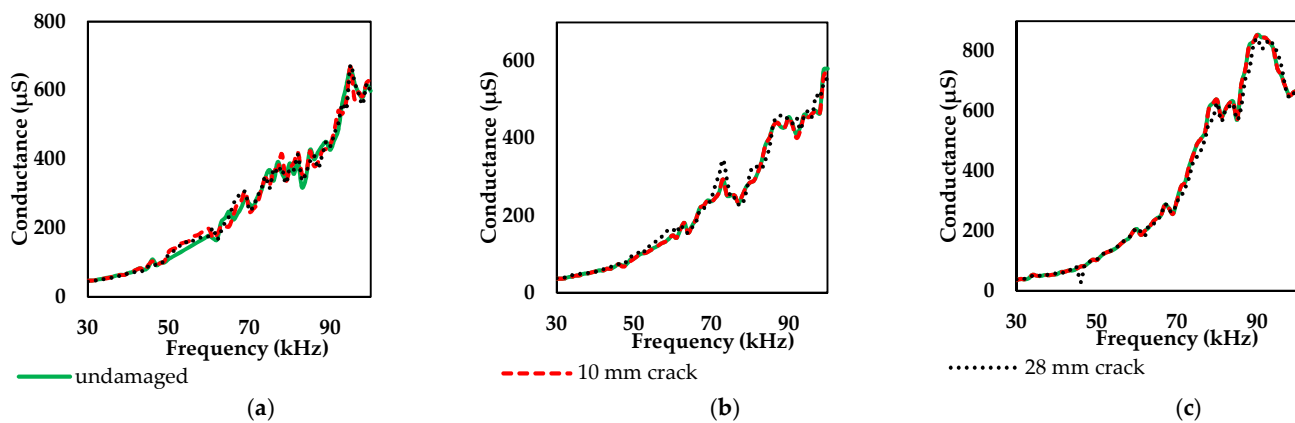


Figure 7. Conductance variations measured for (a) PZT-1; (b) PZT-2; (c) PZT-3 bonded to concrete beam.

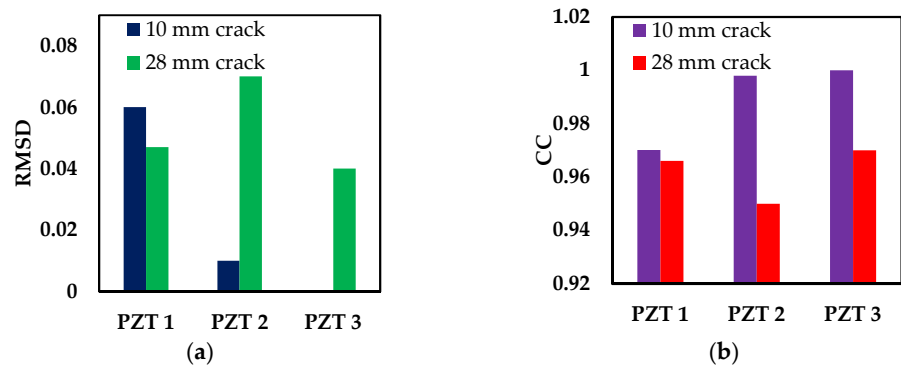


Figure 8. Statistical metrics (a) RMSD; (b) CC evaluated for various PZT sensors.

### 5. Conclusions

The sensors are connected in the parallel/serial connection under Multi-Input Single-Output mode. The trend of experimental results shows a good correlation with the numerical results. The methodology for the damage localization could be verified if different PZT sensors are used. As the experimental studies are based upon a similar type of PZT sensors, the resonant frequencies of PZT sensors could not be differentiated. Different resonant frequencies of each sensor would help localize the structural damage in the concrete structures, as observed in the proposed numerical work. The proposal of the multi-sensing technique on the surface-mounted PZT sensors is recommended for effective SHM.

**Funding:** This research received no external funding.

**Institutional Review Board Statement:**

**Informed Consent Statement:**

**Data Availability Statement:**

**Conflicts of Interest:** The authors declare no conflict of interest.

### References

1. Saravanan, T.J.; Gopalakrishnan, N.; Rao, N.P. Damage detection in structural element through propagating waves using radially weighted and factored RMS. *Measurement* **2015**, *73*, 520–538.
2. Lim, Y.Y.; Bhalla, S.; Soh, C.K. Structural identification and damage diagnosis using self-sensing piezo-impedance transducers. *Smart Mater. Struct.* **2006**, *15*, 987.
3. Annamdas, V.G.M.; Soh, C.K. Three-dimensional electro-mechanical impedance model. II: Damage analysis and PZT characterization. *J. Aerosp. Eng.* **2007**, *20*, 63–71.
4. Saravanan, T.J.; Balamonica, K.; Priya, C.B.; Reddy, A.L.; Gopalakrishnan, N. Comparative performance of various smart aggregates during strength gain and damage states of concrete. *Smart Mater. Struct.* **2015**, *24*, 085016.

5. Saravanan, T.J.; Balamonica, K.; Priya, C.B.; Gopalakrishnan, N.; Murthy, S.G.N. Piezoelectric EMI-based monitoring of early strength gain in concrete and damage detection in structural components. *J. Infrastruct. Syst.* **2017**, *23*, 04017029.
6. Saravanan, T.J.; Balamonica, K.; Priya, C.B.; Gopalakrishnan, N.; Murthy, S.G.N. Non-destructive piezo electric based monitoring of strength gain in concrete using smart aggregate. In Proceedings of the International Symposium Non-Destructive Testing in Civil Engineering (NDT-CE), Berlin, Germany, 5–17 September 2015; pp. 15–17.
7. Bhalla, S.; Kumar, P.; Gupta, A.; Datta, T.K. Simplified Impedance Model for Adhesively Bonded Piezo-Impedance Transducers. *J. Aerosp. Eng.* **2009**, *22*, 373–382.
8. Yang, Y.; Hu, Y.; Lu, Y. Sensitivity of PZT impedance sensors for damage detection of concrete structures. *Sensors* **2008**, *8*, 327–346.
9. Wang, D.; Song, H.; Zhu, H. Numerical and experimental studies on damage detection of a concrete beam based on PZT admittances and correlation coefficient. *Constr. Build. Mater.* **2013**, *49*, 564–574.
10. Wang, T.; Tan, B.; Lu, M.; Zhang, Z.; Lu, G. Piezoelectric Electro-Mechanical Impedance (EMI) Based Structural Crack Monitoring. *Appl. Sci.* **2020**, *10*, 4648.
11. Balamonica, K.; Saravanan, T.J.; Priya, C.B.; Gopalakrishnan, N. Piezoelectric sensor-based damage progression in concrete through serial/parallel multi-sensing technique. *Struct. Health Monit.* **2020**, *19*, 339–356.
12. Saravanan, T.J.; Gopalakrishnan, N.; Priya, C.B. Monitoring of early-age characteristics of concrete using EMI based embedded PZT transducers on varying plate thickness. *Constr. Mater. Syst.* **2017**, 557.
13. Priya, C.B.; Saravanan, T.J.; Balamonica, K.; Gopalakrishnan, N.; Rao, A.R.M. EMI-based monitoring of early-age characteristics of concrete and comparison of serial/parallel multi-sensing technique. *Constr. Build. Mater.* **2018**, *191*, 1268–1284.